

CHAPTER 3

EXPERIMENTAL

3.1. Introduction

The main objectives of this research were to synthesize thermally stable magnetic complexes made up of copper(II) ion, 1,4,8,11-tetraazacyclotetradecane (cyclam; **Figure 3.1**) and alkylcarboxylates ($C_nH_{2n+1}COO$) or arylcarboxylate ($X-C_6H_4COO$ and C_6F_5COO) ions, and to correlate their structures and properties (magnetic and/or liquid crystal) with the values of n and the electronic effect of the substituent(s) on the aromatic ring.

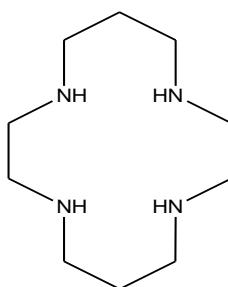


Figure 3.1 The structural formula of cyclam

3.2. Materials

All chemicals and solvents were of analytical grade and used as received without further purification. The list of chemicals used is given in **Table 3.1**.

Table 3.1 The chemicals used in the project, arranged in alphabetical order

Name	Chemical formula	Formula weight (g mol ⁻¹)
<i>p</i> -Aminobenzoic acid	<i>p</i> -H ₂ NC ₆ H ₄ COOH	137.14
Benzoic acid	C ₆ H ₅ COOH	122.12
4,4'-Bipyridine	C ₁₀ H ₈ N ₂	156.18
Copper(II) acetate monohydrate	[Cu(CH ₃ COO) ₂].H ₂ O	199.65
Copper(II) chloride dihydrate	CuCl ₂ .2H ₂ O	170.48
<i>p</i> -Cyanobenzoic acid	<i>p</i> -NCC ₆ H ₄ COOH	147.13
Cyclam	C ₁₀ H ₂₄ N ₄	200.33
Decanoic acid	CH ₃ (CH ₂) ₈ COOH	172.27
Dodecanoic acid	CH ₃ (CH ₂) ₁₀ COOH	200.32
Heptanoic acid	CH ₃ (CH ₂) ₅ COOH	130.18
Hexadecanoic acid	CH ₃ (CH ₂) ₁₄ COOH	256.43
2-Hexyldecanoic acid	CH ₃ (CH ₂) ₇ CH((CH ₂) ₅ CH ₃)COOH	256.43
<i>p</i> -Hydroxybenzoic acid	<i>p</i> -HOC ₆ H ₄ COOH	138.12
<i>p</i> -Methoxybenzoic acid	<i>p</i> -CH ₃ OC ₆ H ₄ COOH	152.15
<i>p</i> -Methylbenzoic acid	<i>p</i> -CH ₃ C ₆ H ₄ COOH	136.15
Octanoic acid	CH ₃ (CH ₂) ₆ COOH	144.21
Pentafluorobenzoic acid	C ₆ F ₅ COOH	212.08
Tetradecanoic acid	CH ₃ (CH ₂) ₁₂ COOH	228.37

3.3. Synthesis

3.3.1. Copper(II)-cyclam-alkylcarboxylates

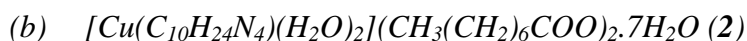
(a) [Cu(C₁₀H₂₄N₄)(H₂O)₂](CH₃(CH₂)₅COO)₂.2H₂O (**1**)

CH₃(CH₂)₅COOH (3.25 g, 25.0 mmol) was added to a minimum volume of aqueous solution of Na₂CO₃ (1.32 g, 12.5 mmol) and the mixture was magnetically stirred and gently heated for about 30 minutes. CH₃(CH₂)₅COONa, formed as a white solid, was

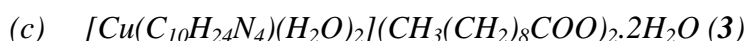
filtered off from the hot mixture and dried overnight in an oven at 60 °C. The yield was 3.62 g (95%).

$\text{CH}_3(\text{CH}_2)_5\text{COONa}$ (2.80 g, 18.4 mmol) was dissolved in hot absolute ethanol (50 ml). $\text{CuCl}_2 \cdot 2\text{H}_2\text{O}$ (1.56 g, 9.2 mmol) was then added to the magnetically stirred hot solution, forming a green powder almost immediately. The reaction mixture was further heated for another 30 minutes. The $[\text{Cu}_2(\text{CH}_3(\text{CH}_2)_5\text{COO})_4]$ formed was filtered under suction, washed with distilled water and dried overnight in an oven at 60 °C. The yield was 2.86 g (97%).

Cyclam (0.50 g, 2.5 mmol) was dissolved in ethanol (50 ml) and the colourless solution was added portionwise to a magnetically stirred hot greenish suspension of $[\text{Cu}_2(\text{CH}_3(\text{CH}_2)_5\text{COO})_4]$ (0.81 g, 1.25 mmol) in ethanol (100 ml). A clear purple solution formed was gently heated for another hour, and then filtered hot. Purple crystals were formed on slow evaporation of the solution at room temperature. The yield was 1.17 g (78%).



The procedure was the same as described in **Section 3.2.1(a)**, using $\text{CH}_3(\text{CH}_2)_6\text{COOH}$ (3.61 g, 25.0 mmol), Na_2CO_3 (1.33 g, 12.5 mmol), $\text{CuCl}_2 \cdot 2\text{H}_2\text{O}$ (1.56 g, 9.2 mmol) and cyclam (0.50 g, 2.5 mmol). The yield of $[\text{Cu}_2(\text{CH}_3(\text{CH}_2)_8\text{COO})_4]$ (green powder) was 3.06 g (95%) and that of **Complex 2** (maroon viscous liquid) was 1.43 g (81%).



The procedure was the same as described in **Section 3.2.1(a)**, using $\text{CH}_3(\text{CH}_2)_8\text{COOH}$ (4.31 g, 25.0 mmol), Na_2CO_3 (1.33 g, 12.5 mmol), $\text{CuCl}_2 \cdot 2\text{H}_2\text{O}$ (1.56 g, 9.2 mmol) and cyclam (0.50 g, 2.5 mmol). The yield of $[\text{Cu}_2(\text{CH}_3(\text{CH}_2)_8\text{COO})_4]$ (green powder) was 3.37 g (90%) and that of **Complex 3** (purple crystals) was 0.91 g (53%).



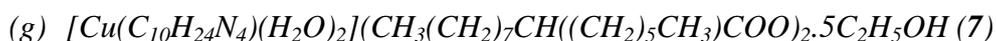
The procedure was the same as described in **Section 3.2.1(a)**, using $CH_3(CH_2)_{10}COOH$ (5.01 g, 25.0 mmol), Na_2CO_3 (1.33 g, 12.5 mmol), $CuCl_2 \cdot 2H_2O$ (1.56 g, 9.2 mmol) and cyclam (0.50 g, 2.5 mmol). The yield of $[Cu_2(CH_3(CH_2)_{10}COO)_4]$ (green powder) was 3.95 g (93%) and that of **Complex 4** (purple crystals) was 1.13 g (61%).



The procedure was the same as described in **Section 3.2.1(a)**, using $CH_3(CH_2)_{12}COOH$ (10.28 g, 45.0 mmol), Na_2CO_3 (2.39 g, 22.5 mmol), $CuCl_2 \cdot 2H_2O$ (2.56 g, 15.0 mmol) and cyclam (0.70 g, 3.5 mmol). The yield of $[Cu_2(CH_3(CH_2)_{12}COO)_4]$ (green powder) was 7.7 g (98 %) and that of **Complex 5** (purple crystals) was 1.78 g (64%).



The procedure was the same as described in **Section 3.2.1(a)**, using $CH_3(CH_2)_{14}COOH$ (6.41 g, 25.0 mmol), Na_2CO_3 (1.33 g, 12.5 mmol), $CuCl_2 \cdot 2H_2O$ (1.56 g, 9.2 mmol) and cyclam (0.30 g, 1.5 mmol). The yield of $[Cu_2(CH_3(CH_2)_{14}COO)_4]$ (green powder) was 4.80 g (91%) and that of **Complex 6** (purple crystals) was 0.98 g (77%).



The procedure was the same as described in **Section 3.2.1(a)**, using $CH_3(CH_2)_7CH((CH_2)_5CH_3)COOH$ (6.41 g, 25.0 mmol), Na_2CO_3 (1.33 g, 12.5 mmol), $CuCl_2 \cdot 2H_2O$ (1.56 g, 9.2 mmol) and cyclam (0.96 g, 4.8 mmol). The yield of $[Cu_2(CH_3(CH_2)_7CH((CH_2)_5CH_3)COO)_4]$ (green powder) was 4.86 g (92%) and that of **Complex 7** (purple viscous liquid) was 3.10 g (62%).

3.3.2. Copper(II)-cyclam-arylcarboxylates

(a) $[Cu(p-H_2NC_6H_4COO)_2(C_{10}H_{24}N_4)].2H_2O$ (**8**)

p-H₂NC₆H₄COOH (6.86 g, 50.0 mmol) was dissolved in ethanol (50 ml), and then gently heated while stirring for 30 minutes, forming a colourless solution. [Cu(CH₃COO)₂].H₂O (4.99 g, 25.0 mmol) was then added portionwise, forming a bluish-green precipitate almost immediately. The reaction mixture was further heated for another 30 minutes. The [Cu₂(*p*-H₂NC₆H₄COO)₄] formed (dark green powder) was filtered under suction, washed with distilled water and dried overnight in a warm oven (60 °C). The yield was 5.95 g (71 %).

Cyclam (0.60 g, 3.0 mmol) was dissolved in ethanol (50 ml), and the colourless solution was added portionwise to a magnetically stirred hot suspension of [Cu₂(*p*-H₂NC₆H₄COO)₄] (1.01 g, 1.5 mmol) in ethanol (100 ml). A clear purple solution formed was gently heated for another hour, and then filtered hot. Purple crystals were formed on slow evaporation of the solution at room temperature. The yield was 0.75 g (47%).

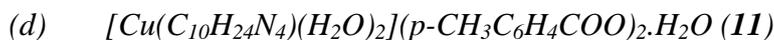
(b) $[Cu(p-HOC_6H_4COO)_2(C_{10}H_{24}N_4)]$ (**9**)

The procedure was the same as described in **Section 3.2.2(a)**, using *p*-HOC₆H₄COOH (13.81 g, 100.0 mmol), [Cu(CH₃COO)₂].H₂O (9.98 g, 50.0 mmol) and cyclam (0.30 g, 1.5 mmol). The yield of [Cu₂(*p*-HOC₆H₄COO)₄] (greenish blue powder) was 7.60 g (81%) and that of **Complex 9** (purple crystals) was 0.19 g (24%).

(c) $[Cu(C_{10}H_{24}N_4)(H_2O)_2](p-H_3COC_6H_4COO)_2.2H_2O$ (**10**)

The procedure was the same as described in **Section 3.2.2(a)**, using *p*-CH₃OC₆H₄COOH (7.61 g, 50.0 mmol), [Cu(CH₃COO)₂].H₂O (4.99 g, 25.0 mmol) and

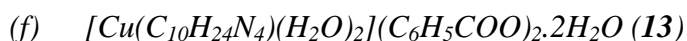
cyclam (0.50 g, 2.5 mmol). The yield of $[\text{Cu}_2(p\text{-CH}_3\text{OC}_6\text{H}_4\text{COO})_4]$ (greenish blue powder) was 8.42 g (92 %) and that of **Complex 10** (purple crystals) was 0.87 g (58%).



The procedure was the same as described in **Section 3.2.2(a)**, using $p\text{-H}_3\text{CC}_6\text{H}_4\text{COOH}$ (6.81 g, 50.0 mmol), $[\text{Cu}(\text{CH}_3\text{COO})_2] \cdot \text{H}_2\text{O}$ (4.99 g, 25.0 mmol) and cyclam (0.50 g, 2.5 mmol). The yield of $[\text{Cu}_2(p\text{-H}_3\text{CC}_6\text{H}_4\text{COO})_4]$ (bluish green powder) was 7.68 g (92%) and that of **Complex 11** (purple crystals) was 0.98 g (67%) .



The procedure was the same as described in **Section 3.2.2(a)**, using $p\text{-NCC}_6\text{H}_4\text{COOH}$ (7.36 g, 50.0 mmol), $[\text{Cu}(\text{CH}_3\text{COO})_2] \cdot \text{H}_2\text{O}$ (4.99 g, 25.0 mmol) and cyclam (0.50 g, 2.5 mmol). The yield of $[\text{Cu}_2(p\text{-H}_3\text{COC}_6\text{H}_4\text{COO})_4]$ (bluish green powder) was 5.28 g (59%) and that of **Complex 12** (maroon crystals) was 0.52 g (37%).



The procedure was the same as described in **Section 3.2.2(a)**, $\text{C}_6\text{H}_5\text{COOH}$ (6.10 g, 50.0 mmol), $[\text{Cu}(\text{CH}_3\text{COO})_2] \cdot \text{H}_2\text{O}$ (4.99 g, 25.0 mmol) and cyclam (0.60 g, 3.0 mmol). The yield of $[\text{Cu}_2(\text{C}_6\text{H}_5\text{COO})_4]$ (blue powder) was 7.18 g (94%) and that of **Complex 13** (purple crystals) was 1.15 g (66%).



The procedure was the same as described in **Section 3.2.2(a)**, using $\text{C}_6\text{F}_5\text{COOH}$ (3.00 g, 14.0 mmol), $[\text{Cu}(\text{CH}_3\text{COO})_2] \cdot \text{H}_2\text{O}$ (1.40 g, 7.0 mmol) and cyclam (0.80 g, 4.0 mmol). The yield of $[\text{Cu}_2(\text{C}_6\text{F}_5\text{COO})_4]$ (blue crystals) was 3.10 g (91%) and that of **Complex 14** (purple crystals) was 1.62 g (53%).

3.4. Instrumental Analyses

The structures of crystalline complexes were deduced by single crystal X-ray crystallography. The structural formulas of non-crystalline complexes were deduced from elemental analyses, Fourier transform infrared spectroscopy (FT-IR), ultraviolet-visible spectroscopy (UV-vis), and room-temperature magnetic susceptibilities by the Gouy method. The thermal stability was determined from thermogravimetric analysis (TGA), and the metallomesogenic properties were deduced by differential scanning calorimetry (DSC) and optical polarizing microscopy (OPM).

3.4.1. X-ray crystallographic data and structural determination

Intensity data for single crystal X-ray diffraction were collected on a Bruker Apex II CCD fitted with graphite monochromated Mo K α radiation ($\lambda = 0.71073 \text{ \AA}$). The intensities were collected using ω -2 θ scan mode. Each data set was corrected for absorption based on multiple scans [1] and reduced using standard methods [2]. All structure were solved by direct method by utilising SHELXS-97 [3] and refined by full matrix least-square methods on F^2 by using SHELXL-97 [3] with anisotropic displacement parameters for non-hydrogen atoms and a weighting scheme of the form $w = 1/[\sigma^2(F_o^2) + aP^2 + bP]$ where $P = (F_o^2 + 2F_c^2)/3$. All hydrogen atoms were refined isotropically in their idealized positions except for water-bound H atoms where they were located in the difference map and were then fixed as in their found position. No absorption corrections were done. The molecular structure of the crystals was drawn with 50 or 70% displacement ellipsoids using Mercury [4].

3.4.2. Elemental analyses

The elemental analyses were performed on a Perkin-Elmer CHNS/O analyser 2400 Series II. The sample was weighed (1-2 mg) in a tin capsule (5x8 mm). The capsule was

folded firmly, and then placed into the analyzer to be heated to a maximum temperature of 1000 °C.

3.4.3. Fourier transform infrared spectroscopy

The Fourier transform infrared spectra (FTIR) were recorded on a Perkin-Elmer Spectrum 400 FT-IR/FT-FIR Spectrometer with attenuated total reflection (ATR) technique or as potassium bromide (KBr) discs on a Perkin-Elmer RX1 FT-IR spectrometer. All spectra were run in the range of 4000-400 cm^{-1} at room temperature.

For the preparation of KBr disc, spectroscopic grade KBr powder was dried in an oven at 120 °C for 12 hours and left to cool in a desiccator. The sample was finely grinded and then mixed with KBr in the mass ratio of about 1:9. The mixture was compressed to a transparent thin disc and then inserted into the spectrometer cell holder. The spectrum obtained was calibrated against KBr as a blank. The peaks were identified by comparison with the corresponding wavenumber from the literature.

3.4.4. Ultraviolet-visible spectroscopy

The ultraviolet-visible (UV-vis) spectra were recorded from 900 – 300 nm on a SHIMADZU UV-vis-NIR 3600 spectrophotometer. The sample was dissolved in ethanol in a 10-mL volumetric flask. The solution was introduced into a 1-cm quartz cuvette and the spectrum was recorded against the solvent as the background, with the following parameter: measuring mode, absorbance; scan speed, fast.

3.4.5. Magnetic susceptibility

The room-temperature magnetic susceptibility was recorded on a Sherwood auto magnetic susceptibility balance. An empty tube was set for tare on the analytical balance and then placed in the instrument. The exponent of the reading was changed to 10^{-5} and was set for tare. The finely grinded sample was packed into the tube to the

calibrated mark and the mass was recorded. The tube containing the sample was then placed in the instrument and the experimental value of χ_g was recorded. The molar magnetic susceptibility (χ_M) was then calculated using the equation: $\chi_M = \chi_g \times M_r$, where M_r was the formula mass of the complex.

3.4.6. Thermogravimetry

The thermogravimetric analysis (TGA) was recorded from 50 – 900 °C on a Pyris Diamond TG/DTA Perkin-Elmer instrument with the scan rate of 20 °C min⁻¹. The sample was analysed under nitrogen at a flow rate of 10 cm³ min⁻¹. An empty ceramic pan was placed in the holder, and then tared. The sample (4 – 5 mg) was loaded onto the pan and the weight was recorded.

3.4.7. Differential scanning calorimetry

The differential scanning calorimetry (DSC) was recorded on a METTLER TOLEDO DSC822 calorimeter. The samples were subjected to two successive heating-and-cooling cycles in the temperature range 30 – 150 °C and scan rate 10 °C min⁻¹. The analysis was performed under nitrogen gas at a flow rate of 10 cm³ min⁻¹. Samples (2–4 mg) in the aluminium crucible was weighed on an external microbalance, and then placed inside the DSC heating stage.

3.4.8. Optical polarizing microscopy

The mesophases were captured using a Nikon-H600L Eclipse Microscope equipped with a Mettler Toledo FP90 central processor and a Linkam THMS 600 hot stage. The heating and cooling rates were 10 °C and 2 °C respectively, and the magnification was 50x.

3.5. Computational methods

All geometry optimizations and frequency calculations were performed at ab initio Hartree – Fock level with 6-311G(d,p) basis set in Gaussian09W package. The electrostatic potentials of the optimized structures were mapped against the elemental charge distribution at isovalue $0.04 \text{ e}/\text{\AA}^3$.

References

- [1] Sheldrick, G. M. (1996). *SADABS*. University of Göttingen, Germany.
- [2] Bruker (2007). *APEX2 and SAINT*. Bruker Axs. Inc., Madison, Wisconsin, USA.
- [3] Sheldrick, G. M. *Acta Crystallogr. Sect. A*: (2008) 64, 112-122.
- [4] Macrae, C. F., Edgington, P. R., McCabe, P., Pidcock, E., Shields, G. P., Taylor, R., Towler, M., van de Streek, J. *J. Appl. Cryst.* (2006) 39, 453-457.